

Exploring the Earth

NORSAR Scientific Report No. 2-2013

## **Semiannual Technical Summary**

1 July – 31 December 2013

Tormod Kværna (Ed.)

Kjeller, June 2014

**NORSAR**

### 6.3 Location of the November 6, 2013, Valdres/Hallingdal Bolide from Infrasound Signals on the NORES Infrasound Array and the NORSAR Seismic Array

#### 6.3.1 Introduction

On November 6, 2013, a fireball was both seen and heard over much of Southern Norway with an estimated time of 19.18.17 UT. The Norwegian Meteor Network (Norsk Meteornettverk, <http://norskmeteornettverk.no/>) collected large numbers of eye-witness accounts and, based upon directions provided by these observers, provided a location estimate somewhat to the West of the town of Fagernes. A preliminary search of the automatic detection list for the NORES infrasound array in Hedmark indicated strong signals shortly after this time coming from the West. An inspection of the seismic traces from the large aperture NORSAR array indicates that many of the seismic sensors also recorded converted acoustic signals. In this short report, I present the observations on these instruments together with an evaluation of how directional estimates from these signals can constrain the location of the event.

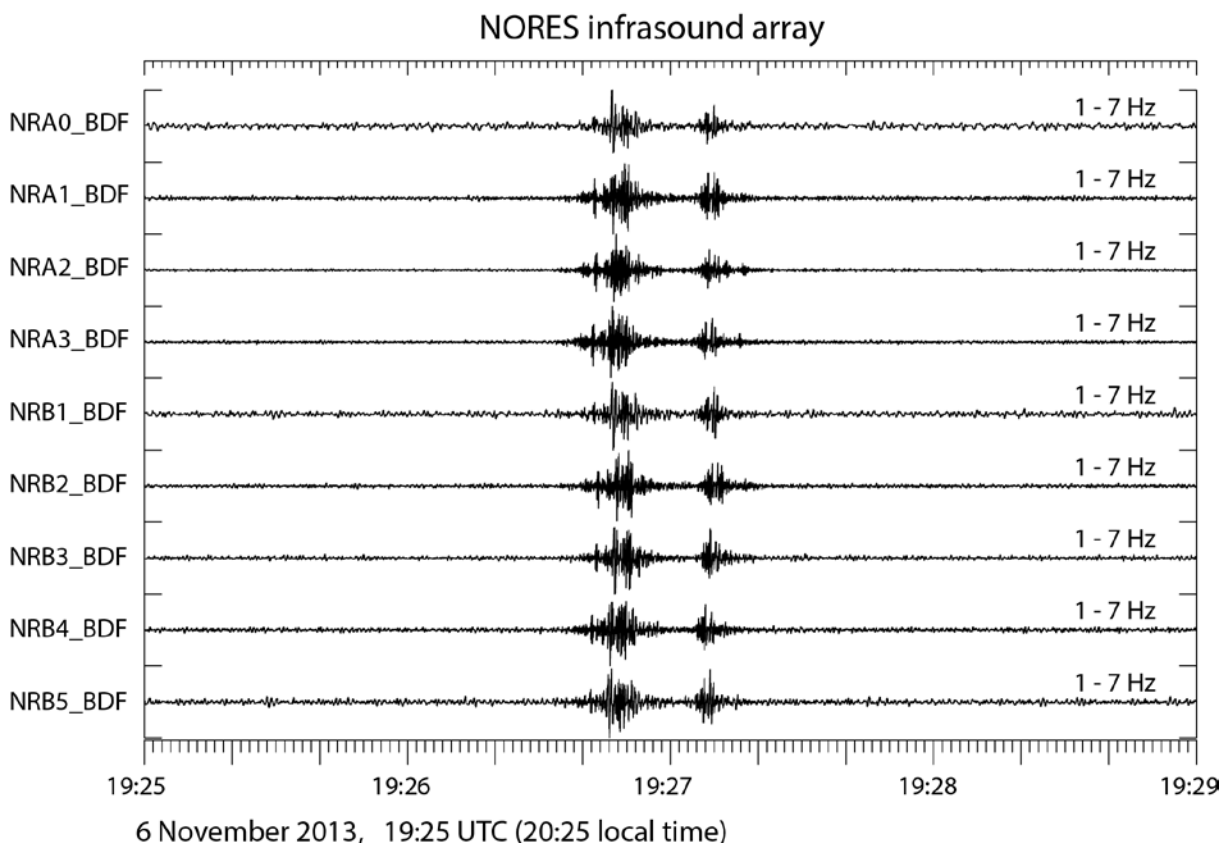


Fig. 6.3.1 Four minutes of microbarograph data from the 9 sensors of the NORES infrasound array bandpass filtered in the 1-7 Hz band.

#### 6.3.2 Observation on the NORES infrasound array

The innermost 9 sites of the NORES seismic array have had infrasound sensors placed in the vaults since April 2013. (A 4-element infrasonic subarray had been running since February 2013.) Details of the array geometry and instrument responses are provided by Roth and Pirli (2013). A four minute data segment, including the signal assumed to be associated with the presumed bolide explosion, is

displayed in Figure 6.3.1. The signal-to-noise ratio (SNR) is good over quite a large range of frequencies (1-10 Hz). There appear to be two major pulses of energy at NORES separated by approximately 25 seconds. The identification of this signal is non-trivial as most of the background noise in the 1-4 Hz band (in which the data is routinely processed) also comes from a similar direction. However, processing overlapping data segments (each of which being 10 seconds long) resulted in the detection of exceptionally coherent signals for a duration of approximately one minute starting at a time 2013-310:19.26.25 with backazimuth estimates between 274 degrees and 279 degrees, and apparent velocity estimates in the range [340 m/s:395 m/s]. A typical slowness grid for this time window is displayed in Figure 6.3.2.

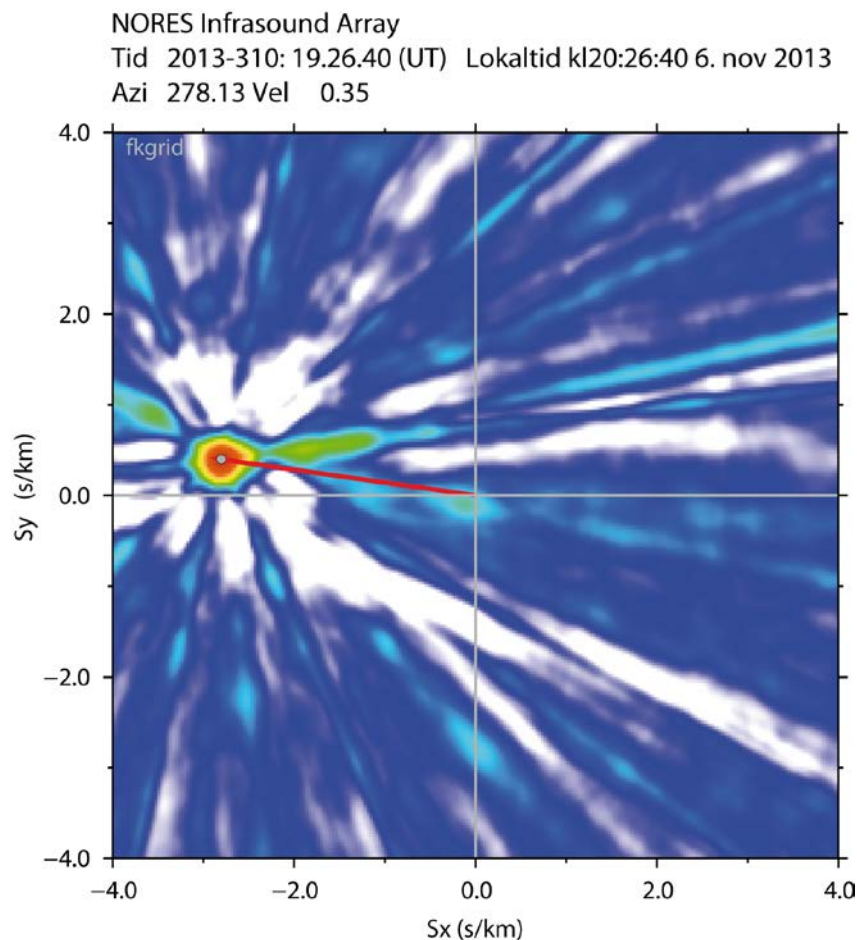


Fig. 6.3.2 Slowness estimate for the infrasound arrival at NORES at the time indicated. The 9 waveforms are bandpass filtered 1-4 Hz prior to parameter estimation, then all pairs of signals are cross-correlated, then the resulting 36 cross-correlation traces are stacked according to the predicted time-delays for a dense grid of slowness vectors. The method is described in more detail by Brown et al. (2002). The coordinates of the center element of the NORES array are  $60.7353^{\circ}\text{N}$ ,  $11.5414^{\circ}\text{E}$ .

### 6.3.3 Observation of Converted Infrasonic to Seismic Signals on the NORSAR Seismic Array

It has long been acknowledged that infrasound can generate a response in seismic sensors. Gibbons et al (2007) demonstrated that the ARCES seismic array in northern Norway had acted as a surrogate infrasound array for almost 20 years - providing excellent records of the acoustic signatures from mining and military explosions in the region - without any of these signals having been classified correctly at the time. The ARCES array has properties that make it quite amenable to the recording of acoustic signals. Firstly, the instruments are all placed in surface vaults, and secondly, the inter-site spacings are small - meaning that acoustic waves above 2 Hz are coherent from sensor to sensor. (Below 2 Hz, the noise generated by ocean waves is usually too high at stations in Fennoscandia for acoustic signals to have an appreciable SNR.) In contrast, the NORSAR array has very large inter-site spacings (with a typical distance of around 5 km between adjacent seismometers) leading to incoherence in the frequency band of interest. The instruments in the NORSAR array are also placed either in boreholes or very large underground vaults, which reduces the possibility of recording atmospheric sound.

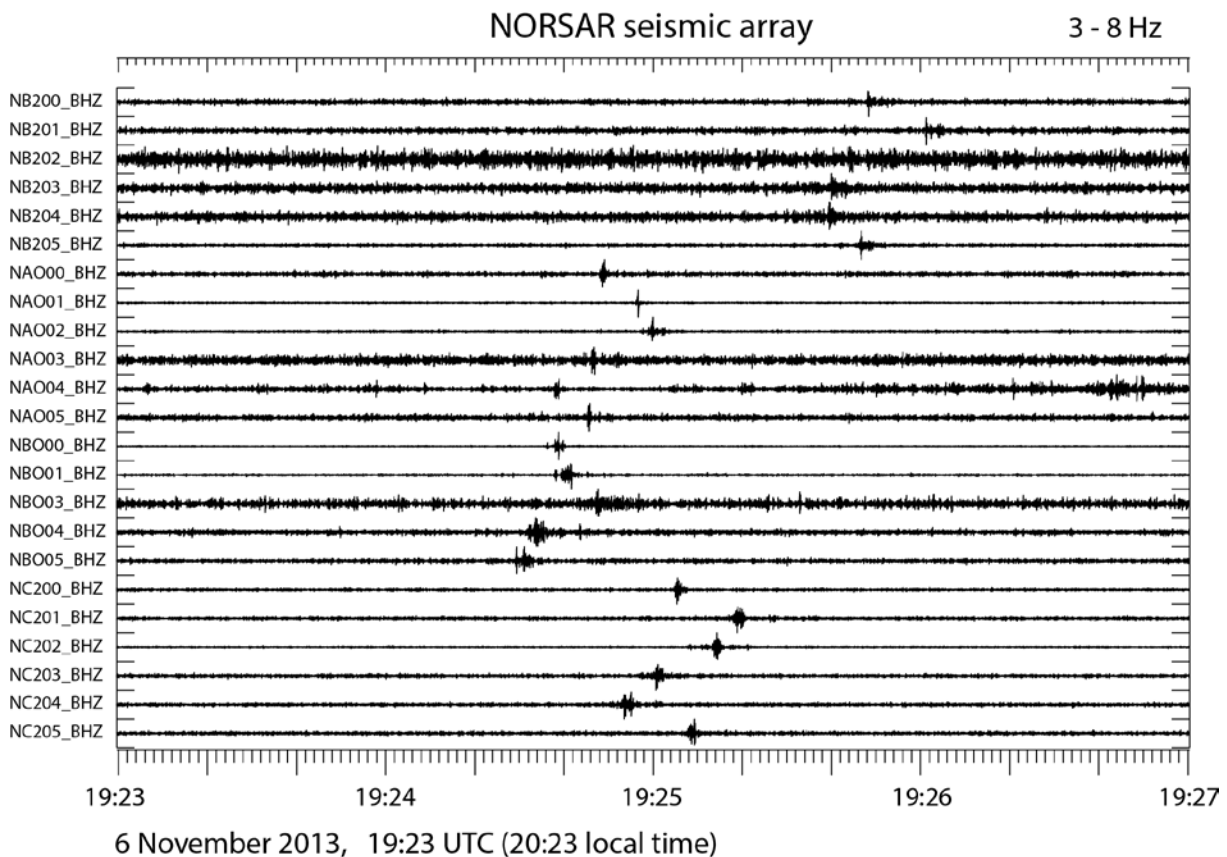


Fig. 6.3.3 Four minutes of waveform data from four subarrays of the large aperture NORSAR (or NOA) seismic array. All waveforms are bandpass filtered 3-8 Hz.

On four of the seven subarrays of NOA short bursts of high frequency energy were well observed, the best signals being observed on the three most westerly subarrays (Figure 6.3.3). The time delay between the acoustic signals on adjacent seismometers is typically longer than the duration of the signals themselves and a rapid inspection of the signals demonstrates that there is not enough waveform similarity for a classical array-processing direction estimator to be applied.

The infrasound community is now realizing that dense deployments of seismometers may provide a far greater spatial representation of the infrasonic wavefield than the limited number of available infrasound arrays (see, for example, Hedlin et al., 2010). This is in spite of the poorer SNR and fidelity to the atmospheric sound signal that the seismometer provides relative to a microbarograph. Hedlin and Walker (2013) advocate the use of reverse time migration (RTM) to be able to locate the sources of infrasound observed over a dense seismic network.

Table 6.3.1 Elements of the NORSAR array at which a time of maximum amplitude for the converted infrasound signal was measured. The times are given in UT in the format ddd:hh.mm.ss.sss where ddd is the Julian day (310 for November 6, 2013), hh, mm, and ss.sss are the hours, minutes and seconds.

Station	Latitude	Longitude	Picked Time of Max. Energy
NB200	61.0397	11.2148	310:19.25.48.168
NB201	61.0495	11.2939	310:19.26.01.580
NB202	61.0069	11.2778	310:19.25.44.815
NB203	61.0107	11.1677	310:19.25.39.599
NB204	61.0498	11.1581	310:19.25.40.530
NB205	61.0710	11.1977	310:19.25.46.677
NAO00	60.8237	10.8324	310:19.24.48.744
NAO01	60.8442	10.8865	310:19.24.56.382
NAO02	60.8057	10.8971	310:19.24.59.921
NAO03	60.7881	10.8084	310:19.24.46.695
NAO04	60.8105	10.7625	310:19.24.38.685
NAO05	60.8507	10.8193	310:19.24.45.578
NBO00	61.0307	10.7774	310:19.24.38.871
NBO01	61.0616	10.7834	310:19.24.41.479
NBO03	61.0129	10.8371	310:19.24.47.440
NBO04	61.0119	10.7524	310:19.24.33.656
NBO05	61.0597	10.7219	310:19.24.29.930
NC200	61.2807	10.8354	310:19.25.05.509
NC201	61.2988	10.9138	310:19.25.18.922
NC202	61.2545	10.9110	310:19.25.14.265
NC203	61.2438	10.8318	310:19.25.00.852
NC204	61.2759	10.7629	310:19.24.54.333
NC205	61.3231	10.8227	310:19.25.09.235

In this case study, it is likely that the size of the observing network, relative to the distance from the source, is sufficiently small that the spread of the wavefield can be approximated well using a circular wavefront model (see Almendros et al., 1999). Given the difference in forms from signal to signal, and the long time needed to propagate over the array (surrogate infrasound network), it appeared that simply estimating the times of the maximum energy on each trace was a sufficient time indicator. Table 6.3.1 provides a list of all of the stations on NOA for which a signal was well observed, together with an estimate of the time of maximum acoustic energy. Setting the reference station to NB200 (the central element of the current NORSAR array) and assuming that the waves all propagate with a horizontal slowness of 2.85 s/km (i.e. 350 m/s) then the iteration prescribed by Almendros et al. with the information provided in Table 6.3.1, results in a backazimuth of 265 degrees and with a distance of approximately 120 km.

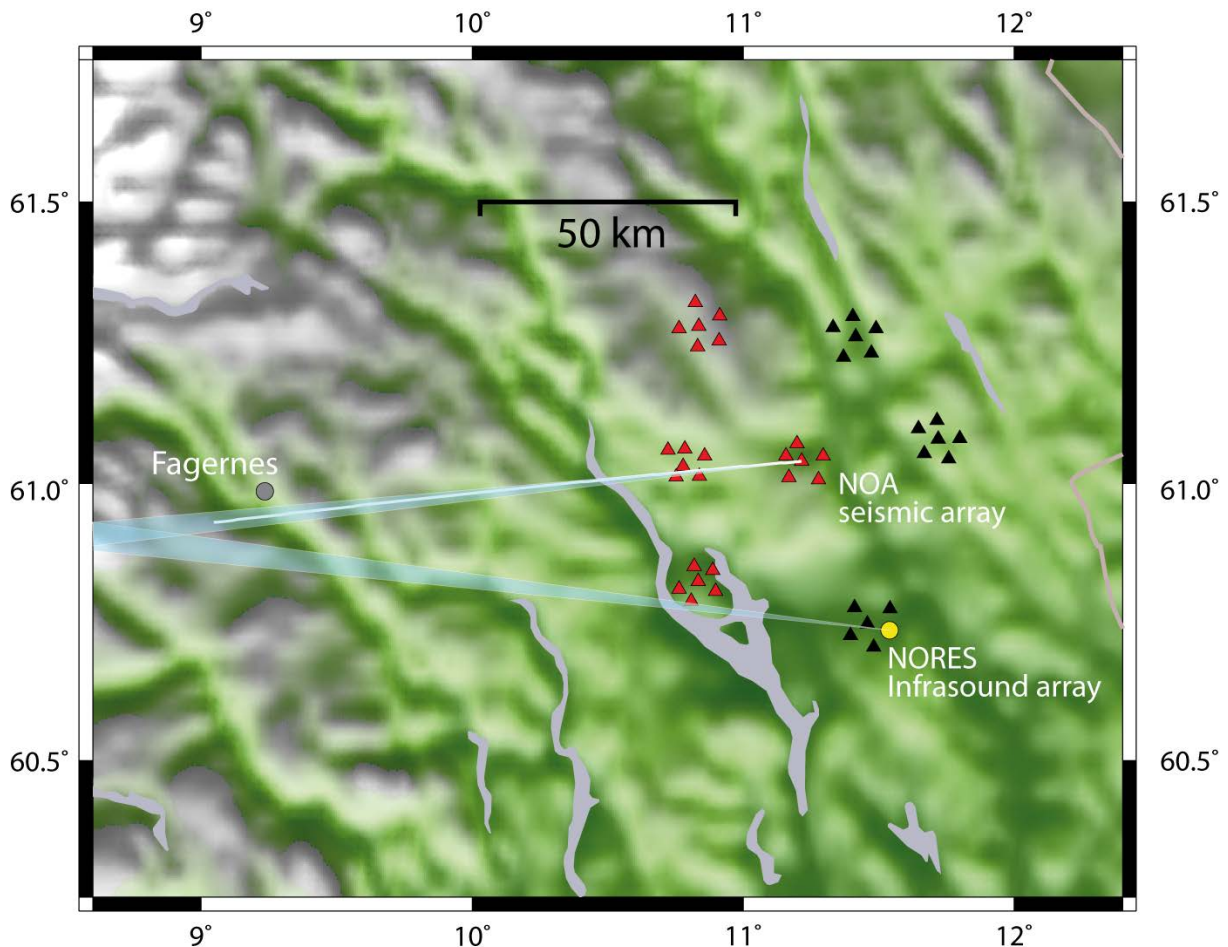


Fig. 6.3.4 Map displaying the location of the NORES infrasound array together with the sites of the NOA (NORSAR) seismic array. Sites with red symbols are those displayed on Figure 6.3.3 which recorded a visible acoustic signal (with the exception of site NBO02 which was not in operation) – the black symbols indicate sites at which no acoustic signals were clearly visible. The blue ray from NORES is a projection of a backazimuth of 278 degrees, and the blue ray from site NB200 of the NOA array is projection of a backazimuth of 265 degrees. The white line marked along this projection has a length of 120 km, the distance from source indicated by the simple curved-wavefield model of Almendros et al. (1999).

#### 6.3.4 Summary

The geometry of the stations, together with the inferred bearings towards the source of the presumed bolide explosion are displayed in Figure 6.3.4. While the station geometry with respect to the source region is poor (the azimuthal gap is very large), the location obtained using a simple bearing between the two different arrays appears to provide a location estimate that is very similar to that inferred from the visual observations (see <http://norskmeteornettverk.no/wordpress/?p=867> - In Norwegian).

## Acknowledgements

I am grateful to Steinar Midtskogen from Norsk Meteornettverk for discussions about this and other similar events.

All plots were generated using the GMT software (Wessel and Smith, 1998).

**Steven J. Gibbons, NORSAR**

## References

- Almendros, J., Ibanez, J. M., Alguacil, G., and E. Del Pezzo (1999). Array analysis using circular-wave-front geometry: an application to locate the nearby seismo-volcanic source. *Geophysical Journal International*, **136**, No. 1. pp. 159-170, [doi:10.1046/j.1365-246x.1999.00699.x](https://doi.org/10.1046/j.1365-246x.1999.00699.x)
- Brown, D. J. , Katz, C. N. , Le Bras, R., Flanagan, M. P., Wang, J., and A. K. Gault (2002) Infrasonic Signal Detection and Source Location at the Prototype International Data Centre, *Pure and Applied Geophysics*, **159**, No. 5., pp. 1081-1125, [doi:10.1007/s00024-002-8674-2](https://doi.org/10.1007/s00024-002-8674-2).
- Gibbons, S. J., Ringdal, F., and T. Kværna (2007) Joint seismic-infrasonic processing of recordings from a repeating source of atmospheric explosions, *The Journal of the Acoustical Society of America*, **122**, No. 5. pp. EL158-EL164, [doi:10.1121/1.2784533](https://doi.org/10.1121/1.2784533)
- Hedlin, M. A. H., Drob, D., Walker, K., and de Groot-Hedlin, C. (2010) A study of acoustic propagation from a large bolide in the atmosphere with a dense seismic network, *Journal of Geophysical Research*, 115, No. B11., B11312, [doi:10.1029/2010jb007669](https://doi.org/10.1029/2010jb007669)
- Hedlin, M. A. H. and Walker, K. T. (2013) A study of infrasonic anisotropy and multipathing in the atmosphere using seismic networks, *Philosophical Transactions of the Royal Society A: Mathematical, Physical and Engineering Sciences*, **371**, No. 1984, [doi:10.1098/rsta.2011.0542](https://doi.org/10.1098/rsta.2011.0542)
- Roth, M. and M. Pirli (2013) Responses of the Infrasound Channels of ARCES and NORES, *Chapter 6.4, NORSAR Scientific Report 2-2012, Semiannual Technical Summary, 1 July – 31 December 2012*, (ed. Tormod Kværna), pp. 59-66.
- Wessel, P. and W.H.F Smith (1998). New, improved version of Generic Mapping Tools released. *EOS, Trans. Amer. Geophys. Union*, **79**, 579.